

Proton Radiography of a Laser-Driven Cylindrical Implosion

R. Jafer¹, L. Volpe¹, D. Batani¹, M. Koenig², S. Baton², E. Brambrink², F. Perez², F. Dorchies³, J.J. Santos³, C. Fourment³, S. Hulin³, P. Nicolai³, B. Vauzour³, K. Lancaster⁴, M. Galimberti⁴, R. Heathcote⁴, M. Tolley⁴, Ch. Spindloe⁴, P. Koester⁵, L. Labate⁵, L. Gizzi⁵, C. Benedetti⁶, A. Sgattoni⁶, M. Richetta⁷, J. Pasley⁸, F. Beg⁹, S. Chawla⁹, D. Higginson⁹, A. MacKinnon¹⁰, A. McPhee¹⁰, Duck-Hee Kwon¹¹, Yongjoo Ree¹¹

¹Università di Milano-Bicocca, Italy

²LULI, Ecole Polytechnique France,

³RAL, STFC, UK

⁴Université de Bordeaux - CNRS - CEA,

⁵CNR Pisa Italy,

⁶University of Bologna Italy,

⁷University of Rome "Tor Vergata" Italy,

⁸University of York UK,

⁹UCSD USA,

¹⁰LLNL, USA

¹¹Korea Atomic Energy Research Institute

Abstract. A recent experiment was performed at the Rutherford Appleton Laboratory (UK) to study fast electron propagation in cylindrically compressed targets, a subject of interest for fast ignition. This experiment was performed in the framework of the experimental road map of the Hiper project (the European High Power laser Energy Research facility Project). In this experiment, protons accelerated by a picosecond laser pulse have been used to radiograph a 220 μ m-diameter, 20 μ m-wall cylinder filled with 0.1 g/cc foam, imploded with ~200 J of green laser light in 4 symmetrically incident beams of pulse length 1 ns. Point projection proton backlighting was used to measure the compression degree as well as the stagnation time. Results were compared to those from hard X-ray radiography. Finally, Monte Carlo simulations of proton propagation in the cold and in the compressed targets allowed a detailed comparison with 2D numerical hydro simulations

Key Words: Laser based proton Radiography, ICF.

INTRODUCTION

Many experiments have been done on Inertial confinement fusion (ICF) and different diagnostics have been used [1] to follow the implosion of the target and measure plasma parameters, one of such diagnostics is Proton Radiography [2-4]. In this context, we performed an experiment at Rutherford Appleton Laboratory (RAL) in the framework of roadmap of the HiPER project [5] in two phases. The goal of the second phase of the experiment was to study the electron transport in cylindrical compressed target. Proton Radiography was used in the first phase to record the implosion history of the cylindrical target. In parallel we used X-ray Radiography to have a comparison. Simulations were made with the Monte Carlo (MC) MCNPX Code [6] using density profiles of the imploded cylinder obtained with the 2D-hydro CHIC code [7,8].

Laser based protons are characterised by small source, high degree of collimation, short duration and a continuous spectrum upto a high-energy cutoff. Taking radiograph with multi-energetic protons allows recording the implosion history in a single shot. Instead x-ray radiograph gives one fluorescent image per laser shot at one fixed time and one has to make several shots in order to reveal the complete history of implosion. Another advantage of using proton radiography is a simple experimental setup keeping imploding cylinder between proton target and proton detector on the same axis.

This paper reports the experimental results as well as the analysis of the most important physical effects involved in proton radiography.

Experimental setup

The experiment was carried out at Vulcan facility using the 100TW, 1ps laser pulse coupled to 4 ns laser beams. The compressed core was probed using protons in order to follow the laser-driven cylindrical implosion. The cylinder was imploded by four long-pulse (LP) laser beams ($\sim 4 \times 50$ J in 1ns) as shown in fig 1(left) at $0.53\mu\text{m}$, focused to $150\mu\text{m}$ FWHM spots.

The $200\mu\text{m}$ long polyimide cylindrical tube with $220\mu\text{m}$ outer diameter and $20\mu\text{m}$ wall thickness was filled with foam (acrylate) at density 0.1 g/cc. One side was closed with a Cu foil and the other with a Ni foil, respectively providing a tracer layer for diagnostics and the source for fast electrons. The Ni foil side was also shielded with a gold cylinder. The four LP beams timing was set so that they hit the target at the same time with precision of ± 50 ps.

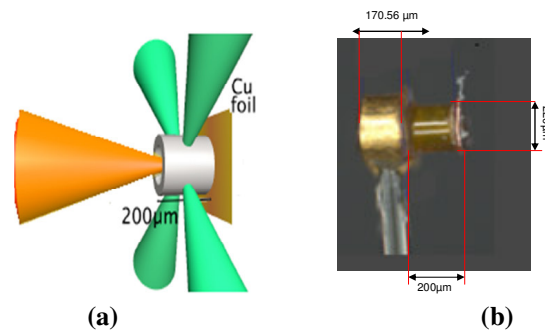


Figure 1. (a) Schematic of the 4 compression beams (each of 1ns) focussed on the plastic cylinder. Also shows the 100TW beam (not used in the first phase of the experiment) propagating along the direction of the cylinder axis (b) Real target fabricated at RAL by M. Tolley and Ch. Spindloe, left side is the gold shielding cylinder and right side is the plastic cylinder filled with low density foam.

A second short pulse beams (SP) (100-150 J in 1ps) was focussed, as a backlighter source, on a $20\mu\text{m}$ thick gold foil, by an $F=3.5$ off axis parabola with a focal spot $10\mu\text{m}$ at FWHM giving a peak irradiance of 1.5×10^{19} W/cm² to produce protons with an approximated exponential spectrum with high energy cut off of about 10MeV.

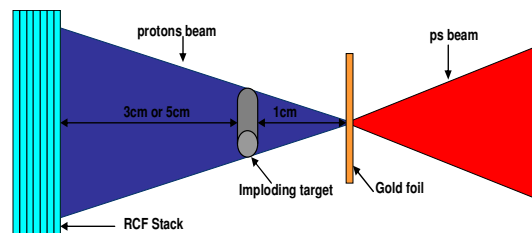


FIGURE 2. Schematic of proton Radiography Setup

The delay, τ , between LP and SP was adjustable between 0 and 3.6ns. The schematic is shown in fig.2.

The proton detector used in this experiment consisted of a multilayer film pack containing spatially resolving radiochromic (RCF) dosimetry film (types: MD-55 and HD- 810). This arrangement, which has been extensively used in laser-driven proton acceleration experiments, gave a diagnostic in which each layer was filtered by the preceding layer, giving a series of images per shot, each corresponding to a different proton energy and hence a different probing time [3].

Experimental results

The experimental radiographs of the reference cylinder as well as of the imploding cylinder at different stages of compressions are shown in fig3. The minimum observed diameter is $\sim 140\mu\text{m}$. Fig 4a shows the comparison between the results of proton radiography (circles) and the predictions obtained with the 2D hydro code CHIC (black dots). Fig 4b shows the comparison between the minimum diameters obtained using x-ray radiography (black dot) and proton radiography (circle). Experimental results show that low energy protons are not able to probe the dense core as deeply as x-rays do as shown in fig 4b.

Although proton radiography data support the same stagnation time ($T=2.1$ ns) of hydro simulations, nevertheless the observed diameter in proton images is always much larger. This can depend on many

physical effects among which the most important are multiple scattering of protons in the target and plasma density and plasma temperature effects affecting the proton stopping power in the target. In order to investigate these physical effects we have run a “start to end” simulation of the process using MCNPX code developed at LANL. In this code the SP and MS effects are taken into account respectively with Bethe [9] and Rossi [10] theories. The simulated radiographs of reference cylinder and of cylinders at different stages of compressions are shown in fig 5.

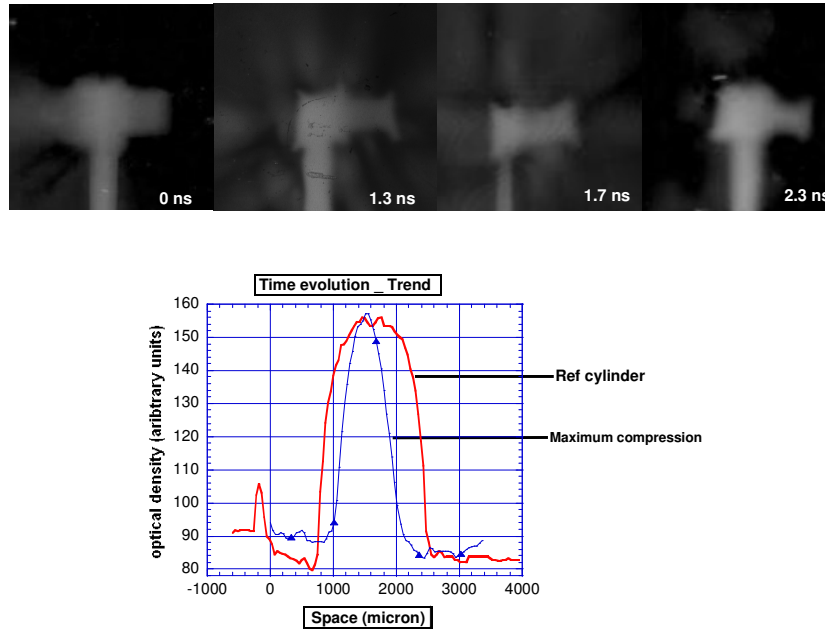


Figure 3. Compression history obtained by experimental proton radiographs (top)s at $t_1=0\text{ns}$, $t_2 = 1.3\text{ns}$, $t_3 = 1.7\text{ns}$, $t_4 = 2.3\text{ns}$.The figure below shows the densitometries along the minimum diameters. The uncompressed plastic cylinder could be fitted with supergaussian (red) while the compressed cylinder (blue) fits with gaussian shape.

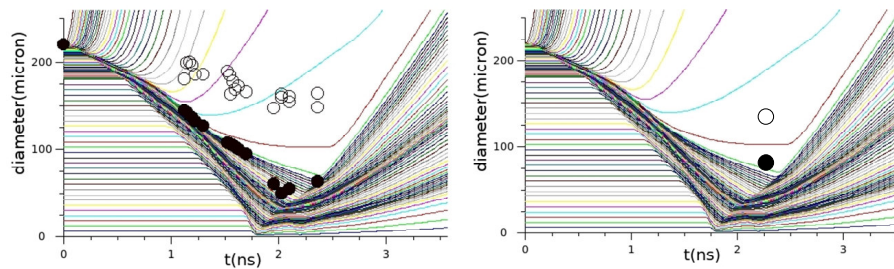


Figure 4. (LEFT) Compression time evolution. Experimental (circles) Vs hydrodynamic simulations (dots).(RIGHT) Proton (circle) Vs X-ray (dot) radiography results, Stagnation time is same as predicted in hydrodynamic simulations but x-rays show large compression than protons. The curves in the above figures show the hydrodynamical evolution of the plastic cylinder at different radial positins.

The code allowed reconstructing “synthetic” proton radiography images starting from the plasma profile given by hydro simulation. Following the experimental analysis we have extracted the FWHM of synthetic images and we got the results shown in fig 6.

As the results were also compared with X-ray radiography, fig 7a shows an obtained image of the imploding cylinder and fig 7b shows the schematic of x-ray radiography setup. Alignments of the ns beams were also crucial for the success of the experiment. An x-ray pinhole camera (PHC) was used to look at the interaction area allowing to check beam alignments. Fig 7c shows the image obtained with PHC superimposed with an exact cross section of the real cylindrical target.

Conclusion

Protons and x-rays have been used to diagnose the implosion of cylindrical targets. X-rays seem more penetrating in compressed targets than low energy protons. Simulations are therefore needed to analyse RCF images.

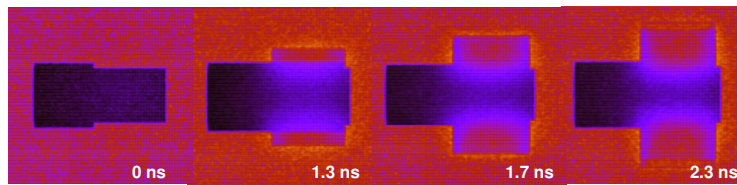


Figure 5. Compression history obtained by simulated proton radiographs at times $t_1=0\text{ns}$, $t_2=1.3\text{ ns}$, $t_3=1.7\text{ns}$ and $t_4=2.3\text{ ns}$

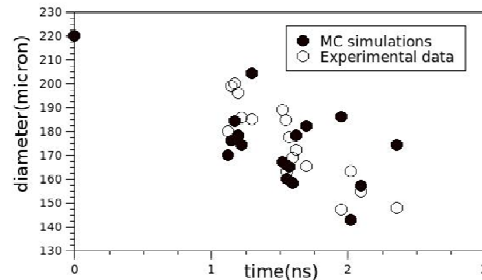


Figure 6. Comparison of experimental results with what are obtained in simulations. The black dot at $220\mu\text{m}$ shows the initial diameter of the cylinder, whereas all other black dots show the simulated compressions. Circles are showing experimental compressions in different shots at different times.

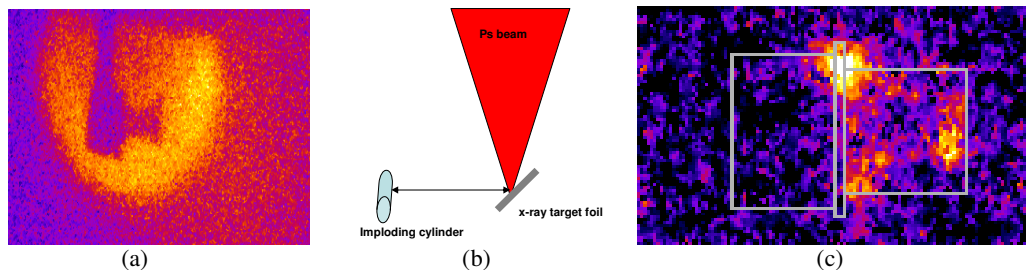


Figure 7.(a) x-ray radiograph (b) schematic of X-ray radiography setup. (c) Image taken from PHC superimposed with cylinder, The PHC was set at 90° from the top in the interaction chamber to look at interaction area. In this image one of the four interaction beam was hitting the Ni foil rather than the plastic cylinder, pointing to beam misalignment.

Simulated data are able to approximately reproduce the observed size of images on RCF experimental data. Taking radiograph with multi-energetic protons allows recording the implosion history in a single shot. The protons do not seem to probe the dense core but the implosion history and the stagnation time is revealed correctly.

ACKNOWLEDGMENTS

The authors gratefully acknowledge the support of the HiPER project and Preparatory Phase Funding Agencies (EC, MSMT and STFC) in undertaking this work.

REFERENCES

- [1] "Advanced Diagnostics for Magnetic and inertial fusion" edited by P.E. Stott, A. Wootton, G. Gorini and D. Batani, Kluwer, Academic/Plenum Publishers, New York ; (2002).
- [2] P.-H. Maire and J. Breil, *Int. J. Num. Meth. Fluids* (bf 56), 1417 (2008).
- [3] A.J.Meckinonn et al. *Phy. Rev. Let.* 97,045001(2006).
- [4] M.Borghesi et al. *Plasma physics. Control. Fusion* 43(2001) A267-A276.
- [5] www.hiper-laser.org (the European High Power laser Energy Research facility Project)
- [6] <https://mcnpx.lanl.gov>
- [7] C. K. Li at al. *Phy. Rev. Let.* 100, 225001 (2008).
- [8] P.-H. Maire, J. Breil, R. Abgral, and J. Ovadia, *SIAM SISC*, 1781 (2007).
- [9] G. Moliere, *Z. Naturfosh*, 2a (1947) 133; 3a (1948) 78. H. A. Bethe, *Phys. Rev.* 89 (1953) 1256. W.T.Scott, *Rev. Mod.*
- [10] B. Rossi and K. Greisen *Rev. Mod. Phys* 13 (1941).